The Hepatic Microcirculation in the Isolated Perfused Human Liver

Jean-Pierre Villeneuve,[1] Michel Dagenais,[2] P-Michel Huet,[1] André Roy,[2] Réal Lapointe,[2] and Denis Marleau[1]

In cirrhosis, capillarization of sinusoids could result in impaired exchanges between the hepatocytes and the blood perfusing the liver and contribute to liver failure irrespective of the metabolic capacity of the liver. To characterize anomalies of the hepatic microcirculation, we used the multiple-indicator dilution approach in isolated perfused livers obtained from patients with cirrhosis at the time of transplantation, and from organ donors with normal or near-normal livers or hepatic steatosis. In organ donors, the sinusoidal volume and the permeability of sinusoids to albumin, sucrose, and water were found to be comparable to that of normal dog and rat livers. The sinusoidal volume and the extravascular volume (EVV) accessible to diffusible tracers were larger after hepatic artery than after portal vein injection, probably because of an unshared arterial sinusoidal bed. In cirrhotic livers, two kinds of alterations were found: the appearance of a barrier between the sinusoids and the hepatocytes (capillarization) and intrahepatic shunts. The extravascular space accessible to albumin decreased with increasing severity of cirrhosis, and the diffusion of sucrose in the space of Disse showed a barrier-limited pattern, instead of the normal flow-limited behavior. In cirrhotic livers, a correlation was found between the hepatic extraction of indocyanine green (ICG) and the extravascular space accessible to albumin ($r = .84$, $P < .05$), suggesting that the impaired access of this protein-bound dye to the hepatocyte surface contributed to its impaired elimination. Intrahepatic shunts were found between portal and hepatic vein (21% ± 16% of portal flow), but not between hepatic artery and hepatic veins. We conclude that (1) the behavior of diffusible tracers in human livers with normal liver architecture is comparable to that reported in normal animals; (2) the permeability of sinusoids in cirrhotic livers is abnormal, (3) permeability changes are related to changes in liver function in cirrhosis. (Hepatology 1996;23:24-31.)

The cause of hepatic failure in cirrhosis remains unclear. Hepatic failure may become manifest when the liver and hepatocyte volume is only moderately decreased. We have proposed that anomalies of the hepatic microcirculation could result in impaired exchanges between the hepatocytes and the blood perfusing the liver and thus contribute to liver failure irrespective of the metabolic capacity of hepatocytes ("intact cell hypothesis").[1] A striking change during cirrhosis is the transformation of the hepatic sinusoids (discontinuous capillaries) into continuous capillaries.[2-4] Capillarization leads to a restriction in the diffusion of albumin and albumin-bound substrates from the plasma to the interstitial space (space of Disse). We and others have documented these anomalies in a rat model of cirrhosis induced by repeated administration of carbon tetrachloride[5-8] and in human cirrhosis.[9]

In the current study, using a procedure developed to perfuse cirrhotic human livers obtained from liver transplantation patients, we examined the hepatic microcirculation in normal or near-normal human livers obtained from organ donors in whom the liver was considered not suitable for liver transplantation, and compared them with cirrhotic livers. The microcirculation was characterized with the multiple indicator dilution approach,[10] which provides a way to probe the permeability properties of hepatic sinusoids and capillaries.

PATIENTS AND METHODS

Liver Procurement. Normal or near-normal livers were obtained from six organ donors in whom the liver was considered not suitable for liver transplantation: two had abnormal liver function tests after cardiopulmonary resuscitation, one was hepatitis B surface antigen positive with normal liver enzymes (this later turned out to be a false-positive result), two had hepatic steatosis (20% and 50% of hepatocytes, respectively) and one had anatomic variations that made arterial reconstruction impossible. Cirrhotic livers were obtained from 10 patients who underwent orthoptic liver transplantation. Data from 8 of the 10 cirrhotic livers were reported in part in a previous publication.[11] Clinical and biochemical data in the 16 subjects studied are summarized in Table 1. The study was approved by our institution's ethics committee; written informed consent was obtained from each patient before transplantation, and from the family in the case of organ donors.

Abbreviations: RBC, red blood cells; MS, microspheres; AUC, area under the curve; EVV, extravascular volume; ICG, indocyanine green.

From the Department of [1]Medicine and [2]Surgery, Centre de recherche clinique André-Viallet, Hôpital Saint-Luc and Université de Montréal, Montreal, Quebec, Canada.

Received November 25, 1994; accepted July 25, 1995.

Supported by grant no. PG-1118 of the Medical Research Council of Canada, Ottawa, Canada.

Address reprint requests to: Jean-Pierre Villeneuve, MD, Centre de Recherche Clinique André-Viallet, 264 René-Levesque East, Montreal, Québec, Canada.

0270-9139/96/2301-0004$3.00/0

TABLE 1. Clinical and Biochemical Data in Organ Donors and Patients With Cirrhosis

Case	Diagnosis	Age (yr)	Bilirubin (μmol/L)	Albumin (g/L)	Prothrombin Time (sec above control)	AST (IU/L)	ALT (IU/L)	Pugh Score	Portohepatic Gradient (mm Hg)*	ABT (%)†	Interval Between Ligature of Hepatic Vessels and Liver Perfusion (hr)
Organ donor 1		21	13	28	—	25	12	—	—	—	11.0
Organ donor 2		21	19	—	4.1	521	428	—	—	—	1.5
Organ donor 3		14	5	—	10.0	79	51	—	—	—	14.0
Organ donor 4		52	19	—	—	31	54	—	—	—	13.0
Organ donor 5		61	7	—	0	13	9	—	—	—	6.0
Organ donor 6		66	12	45	1.3	67	238	—	—	—	6.5
Cirrhosis 1	PBC	38	187	33	0.0	76	37	8	7	16.6	2.5
Cirrhosis 2	Cryptogenic	55	51	29	8.0	76	34	11	—	1.3	3.0
Cirrhosis 3	PBC	59	493	22	3.0	212	136	10	—	4.2	2.5
Cirrhosis 4	PBC	58	221	33	2.0	191	119	9	—	12.4	2.0
Cirrhosis 5	CAH-AI	39	485	15	1.5	37	49	10	22	1.6	1.0
Cirrhosis 6	Wilson	21	343	20	15.0	232	183	13	14	0.5	2.0
Cirrhosis 7	CAH-C	38	85	25	5.5	65	37	14	27	1.8	2.0
Cirrhosis 8	Alcoholic	50	107	24	5.5	48	14	11	25	—	3.0
Cirrhosis 9	Alcoholic	45	116	25	8.5	91	36	13	23	0.9	17.0
Cirrhosis 10	CAH-B	56	221	18	4.5	64	34	12	—	0.6	2.0

Abbreviations: ABT, aminopyrine breath-test; CAH-AI, chronic active hepatitis, auto-immune; PBC, primary biliary cirrhosis; CAH-B, chronic active hepatitis, hepatitis B virus; CAH-C, chronic active hepatitis, hepatitis C virus.

* Portohepatic gradient was measured as free portal vein or wedged hepatic vein pressure minus free hepatic vein pressure.

† Results are expressed as percent of dose excreted in 2 hours; the normal value in our laboratory is 9.3% (95% confidence interval = 5.6 to 12.8%).

Liver Perfusion. For organ donors, the liver was flushed with UW-2 solution through the aorta and portal vein, removed, and stored on ice according to standard liver procurement technique. For cirrhotic patients, the liver was removed *en bloc,* flushed with 1.5 L of ice-cold lactated Ringer's solution, and kept on ice until connected to the perfusion apparatus. In the last two cirrhotic livers, livers were flushed with UW-2 solution instead of Ringer's solution, to minimize ischemic injury. The interval between ligature of hepatic vessels in the operating room and connection of the liver to the perfusion apparatus averaged 5 hours, ranging from 1 to 17 hours (Table 1).

The livers were perfused through the hepatic artery and portal vein, in a closed recirculating system, as previously described.[11] The perfusate consisted of 1.5 to 2.0 L of Krebs bicarbonate buffer containing 20% (vol/vol) prewashed human or bovine red blood cells (RBC), 20 g/L bovine serum albumin, 2 g/L α_1-acid-glycoprotein, 2.1 mmol/L calcium, and 5.5 mmol/L glucose. Portal vein and hepatic artery flows were set to obtain perfusion pressures similar to those anticipated *in vivo.* Portal vein and hepatic artery pressures were measured with strain-gauge transducers. Portal vein resistance ($dyn \cdot s \cdot cm^{-5} \cdot 10^3$) was calculated as: portal pressure (mm Hg) × 80/portal flow (mL/min). Hepatic artery resistance was calculated as: hepatic artery pressure × 80/hepatic artery blood flow. During the perfusion, bile output, blood gases, and pH, electrolytes, glucose, and liver enzymes were measured at regular intervals. At the end of each experiment, biopsies were performed for histological examination.

Indicator Dilution Curves. After 20 minutes of stabilization, multiple indicator dilution curves were carried out as previously reported in the rat.[8] The injection mixture consisted of ^{51}Cr-labeled RBC (0.5 μCi), ^{99}Tc-albumin (0.5 μCi), [^{14}C]sucrose (3.0 μCi), and $^{3}H_2O$ (6.0 μCi). The hematocrit, albumin, and α_1-acid-glycoprotein concentrations of the bolus were matched to those of the perfusate. The injection mixture was placed in a 1.0 mL flow-through cuvette and rapidly flushed into the portal vein. A PE-90 polyethylene tubing (Clay-Adams, Parsippany, NJ) was placed in a right or left hepatic vein, and samples were collected in serial tubes at a rate of 1 tube per second for 90 seconds. During sample collection, the perfusion circuit was diverted on the effluent side to prevent recirculation. A second set of dilution curves was obtained after injection of a mixture containing ^{51}Cr-labeled RBC (0.5 μCi) and ^{141}Ce-labeled 15 μm microspheres (MS) (0.5 μCi; 10,000 beads) in portal vein. The microspheres were sonicated for 15 minutes at 40°C before injection. In the six organ donors and in six of the cirrhotic patients, similar sets of dilution curves were obtained after injection of the same boluses in the hepatic artery, with sampling in the hepatic vein.

The samples were counted as previously described.[8] The outflow activity (dpm per mL) was divided by the amount injected (dpm) to provide a basis for comparison between the tracers, yielding a pattern expressed in terms of the outflow fraction per milliliter of blood (i.e., a reciprocal volume).[10] Linear extrapolation of the downslope to infinity was carried on a semilogarithmic plot and the areas under the outflow fraction/time curves (AUC) were calculated.

Data Analysis. Data were analyzed according to the flow-limited distribution model of Goresky.[10] According to the model, the peak concentration (C) of diffusible labels (diff) in the outflow is reduced by a factor $1/(1 + \gamma)$ relative to that of RBC, and their transit time (t) is increased by the factor $1 + \gamma$, on the basis of the relationships:

$$C_{diff} = C_{RBC}/(1 + \gamma) \quad (1)$$

and

$$t_{diff} - t_0 = (t_{RBC} - t_0)*(1 + \gamma) \quad (2)$$

where t_0 is the transit time through nonexchanging vessels

(catheter, portal vein, and hepatic veins). The diffusible label curve, when adjusted in time by a factor $1/(1 + \gamma)$ and adjusted in concentration by the factor $(1 + \gamma)$, should superimpose on the RBC curve.

The diffusible label curves were analyzed by an iterative nonlinear least squares method[12] to make them superimpose on the RBC curve, yielding estimates of $1 + \gamma$, and t_0. The optimization procedure was continued until the sum of squares of the deviations changed by less than 0.1% from one iteration to the next. The result of the fitting procedure was evaluated by visual inspection of the fitted curve and by measuring the coefficient of variation and the coefficient of determination of the fit.[13] The mean transit time of each label was calculated using the method of Meier and Zierler,[14] and t_0 was subtracted from these values to provide estimates of the mean transit time of the labels through the sinusoids (t).

The distribution space for each label, V, was determined as the product of the mean transit times (t) and the appropriate flow rates, Q:

$$V = Q*t \quad (3)$$

Sinusoidal blood volume, albumin, and sucrose distribution spaces and water space were estimated by use of the respective blood (Q_B), plasma (Q_P), and water flows (Q_W). The water flow was calculated as:

$$Qw = [Q*Ht*0.70] + [Q*(1 - Ht)*0.93] \quad (4)$$

where Ht is the hematocrit, and 0.70 and 0.93 represent the proportion (v/v) of the RBC and plasma phases made up by water.[15]

The extravascular volumes (EVV) accessible to diffusible tracers (albumin, sucrose, and water) were calculated as model-independent parameters using the transit time method as follows:

$$EVV_{diff} = Q_{diff}*(t_{diff} - t_{rbc}) \quad (5)$$

where t_{diff} is the transit time of diffusible labels and Q_{diff} is the plasma flow (for albumin and sucrose) or the water flow (for water).

Intrahepatic shunts (percentage) were calculated as: $(AUC_{MS}/AUC_{RBC}) \times 100$. In the presence of intrahepatic shunts, the recovery of RBC and of diffusible tracers in the outflow can be viewed as consisting of two parts, with part of the material flowing through shunts, and another part flowing through more normal sinusoids lined by hepatocytes. To assess the sinusoidal volume and the behavior of diffusible labels, the microspheres curve was therefore subtracted from each tracer curve before analysis in cases with intrahepatic shunting.

Indocyanine Green (ICG) Clearance and Extraction. ICG (15 mg) was injected as a bolus in the reservoir, and samples were obtained from the reservoir at 5-minute intervals for the next 30 minutes. ICG concentrations were measured by spectrophotometry.[16] ICG kinetic was analyzed according to a one-compartment open model. The clearance of ICG was estimated from the area under the perfusate concentration-time curve extrapolated to infinity (AUC) as: Clearance = Dose/AUC. The ICG hepatic extraction ratio (E) was calculated as: E = clearance/perfusate flow.

Statistics. Results are expressed as mean ± SD. Means were compared with Student's *t*-test for paired or unpaired data. Correlation was assessed by least-squares regression analysis. A *P* value less than .05 was considered significant.

TABLE 2. Isolated Perfused Human Livers: Perfusion Characteristics

	Organ Donors (n = 6)	Cirrhosis (n = 10)
Duration of perfusion (min)	273 ± 42	285 ± 70
Liver weight (g)	1,697 ± 171	1,491 ± 385
Portal vein flow (mL/min)	783 ± 90	368 ± 148*
Hepatic artery flow (mL/min)	283 ± 114	100 ± 83*
Total hepatic flow		
· mL/min	1,067 ± 160	468 ± 135*
· mL/min/g liver	0.632 ± 0.098	0.331 ± 0.143*
Portal vein pressure (mm Hg)	6.5 ± 1.8	20.4 ± 9.5*
Hepatic artery pressure (mm Hg)	49 ± 17	54 ± 21
Portal vein resistance $(dyn \cdot s \cdot cm^{-5} \cdot 10^3)$	0.68 ± 0.27	5.7 ± 4.1*
Hepatic artery resistance $(dyn \cdot s \cdot cm^{-5} \cdot 10^3)$	17.2 ± 11.2	41.1 ± 23.6
Oxygen consumption (μmole/min/g liver)	0.758 ± 0.202	0.465 ± 0.190*
ALT release (IU/min)	1.0 ± 0.7	1.4 ± 1.6

NOTE. Results are expressed as mean ± SD.
* $P < .05$ compared with organ donors.

RESULTS

Histology and Liver Perfusion. Histological examination showed a normal liver architecture in organ donors and confirmed the presence of cirrhosis in the cirrhotic group. The descriptive features of the liver perfusions are summarized in Table 2. In organ donors' livers, perfusion flow was set at approximately 1 L/min, with 75% coming from the portal vein and 25% from the hepatic artery. This resulted in pressures similar to those observed *in vivo* in normal humans. In cirrhosis, intrahepatic portal vein resistance was markedly increased, resulting in higher portal pressures at lower flow values. Attempts to increase portal flow in cirrhosis resulted in liver swelling and inappropriately high portal pressure. Throughout the perfusion, gross appearance, oxygen consumption, portal and hepatic artery pressures, and bile flow remained stable, but there was an increase in alanine transaminase concentration in the reservoir (Fig. 1 and Table 2).

Intrahepatic Shunts. Indicator dilution curves with RBC and MS demonstrated the absence of shunts larger than 15 μm in diameter from portal vein or hepatic artery to hepatic veins in organ donors' livers (Table 3). In cirrhotic livers, shunts from the portal vein to the hepatic veins were found in 9 of 10 cases, ranging from 1.2% to 59.2% of portal flow. After hepatic artery injection, a small amount of MS was recovered in the outflow in two cases, but the microspheres did not have the profile of a dilution curve.

The presence of intrahepatic shunts resulted in bimodal outflow curves for labeled RBC, albumin, sucrose, and water, with an early component related in time to the peak of microspheres, and a later component corresponding to label that had passed through a more normal part of the vascular bed. This phenome-

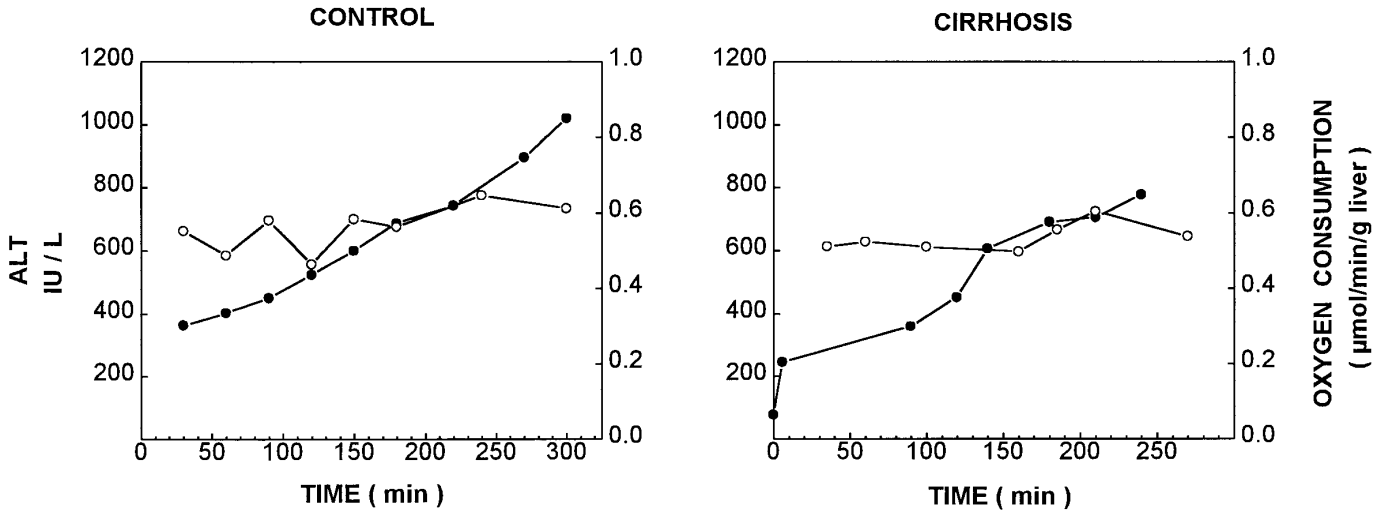

FIG. 1. Representative examples of oxygen consumption (—○—) and ALT concentration (—●—) in the reservoir during perfusion of isolated human livers.

non was apparent on inspection of the dilution curves in cases with a large amount of shunts, and was seen as a shoulder on the upslope of the RBC, albumin, and sucrose curves (Fig. 2). It was most obvious for the water curve, with a sharp early peak related in time to the MS curve. After subtraction of the MS curve from each tracer, the curves then exhibited the usual form that one would expect to see for indicators passing through more normal sinusoids.

Labeled Indicator Studies. A typical set of dilution curves for RBC, albumin, sucrose, and water in an organ donor is shown in Fig. 3. The pattern was similar to that reported in normal dogs and rats.[8,17] The labeled RBCs emerged first, their curve reached the highest and earliest peak, and decayed most quickly. Albumin and sucrose showed a progressive delay in their outflow appearance, a lower peak, and a progressively decreasing rate of downslope decay. Changes for the water curve were similar to those of albumin and sucrose, but more pronounced, as water enters the hepatocytes and diffuses in a larger space of distribution. Results of sinusoidal volume and EVV calculations are shown in Fig. 4. Because values in normal humans are not available, data in normal rats were used as a basis for comparison. In organ donors, the distribution space of RBC and the distribution space of diffusible tracers relative to that of RBC were within the range reported in normal rats. As expected in the delayed wave flow–limited case, the diffusible label curves could be transformed to superimpose on the RBC curve (Fig. 5).

Dilution curves in cirrhotic patients differed from organ donors (Figs. 3 and 4). The sinusoidal volume was decreased in 8 of 10 cases. The distribution of albumin, sucrose, and water showed three different patterns. In four cases (cases 1 to 4 in Table 1), the diffusion of albumin in the space of Disse was normal, but the relative extravascular space accessible to sucrose was increased. In these cases, the shape of the albumin curve was normal, but the sucrose curve was biexponential with a delayed downslope. The fit of the transformed sucrose curve over that of RBC was not good (Fig. 5). The extravascular volume accessible to water was also increased.

A second pattern was observed in five other cases (cases 5 to 9 in Table 1). In these patients, the labeled albumin curve reached a higher and earlier peak and tended to superimpose on the RBC curve. The extravascular volume accessible to albumin was decreased, indicating a restriction in the diffusion of albumin, as can be found in a capillary circulation. The labeled albumin

TABLE 3. Assessment of Intrahepatic Shunts After Portal Vein and Hepatic Artery Injection of Radiolabeled Microspheres and Red Blood Cells

Case	Portal Vein to Hepatic Vein Shunts (% of flow)	Hepatic Artery to Hepatic Vein Shunts (% of flow)
Organ donor 1	0.0	0.0
Organ donor 2	0.0	0.0
Organ donor 3	ND	ND
Organ donor 4	0.0	0.0
Organ donor 5	0.0	0.0
Organ donor 6	0.0	0.0
Cirrhosis 1	0.0	ND
Cirrhosis 2	21.0	0.0
Cirrhosis 3	25.4	ND
Cirrhosis 4	1.2	1.2
Cirrhosis 5	9.8	ND
Cirrhosis 6	28.1	0.0
Cirrhosis 7	32.2	ND
Cirrhosis 8	10.7	0.0
Cirrhosis 9	59.2	1.1
Cirrhosis 10	14.9	0.0

Abbreviation: ND, not determined.

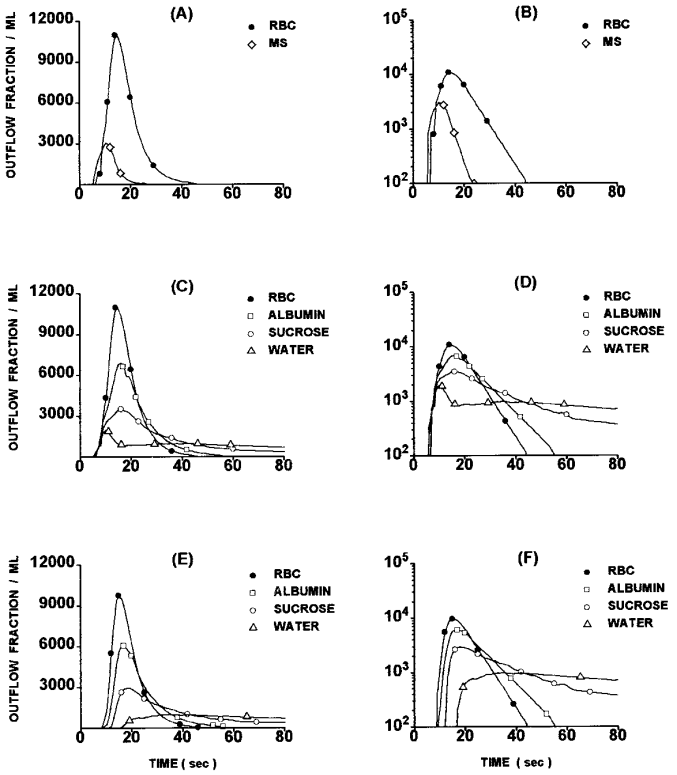

FIG. 2. Indicator dilution curves in a cirrhotic liver with intrahepatic shunting from the portal vein to the hepatic vein (case 6) (A) Red blood cells (RBC) and microspheres (MS) curves, linear ordinate scale: 28% of microspheres injected are recovered in the outflow. (B) Same as (A), logarithmic ordinate scale. (C) RBC, albumin, sucrose, and water curves, linear ordinate scale: a shoulder is seen on the upslope of the RBC, albumin, and sucrose curve, and an early peak is seen on the water curve, related in time to the MS curve. (D) Same as (C) logarithmic ordinate scale. (E) Same as (C), but after subtracting the microspheres curve from each tracer curve, linear ordinate scale: the curves now exhibit the usual form expected for diffusible labels. (F) Same as (E), logarithmic ordinate scale.

curve, when transformed, nevertheless superimposed on the RBC curve, and its diffusion therefore appeared compatible with a flow-limited kind of behavior. In these cases, the extravascular space accessible to sucrose was normal, but the downslope of the sucrose curve was biexponential, and the fit of sucrose over RBC was poor. Similar to sucrose, the extravascular space accessible to water was normal in four of five cases.

In the last case (case 10 in Table 1), both the albumin and sucrose curves tended to superimpose on the RBC curve, and their extravascular volumes were decreased.

Portal Vein Versus Hepatic Artery Studies. Comparison of results obtained after injection of indicators in the portal vein and hepatic artery is shown in Fig. 6. In organ donors, the sinusoidal volume and the extravascular volume accessible to albumin, sucrose, and water was larger after hepatic artery than after portal vein injection. In cirrhotic livers, the sinusoidal volume was similar with both routes of injection, but the EVV of diffusible indicators was larger after hepatic artery injection.

ICG Extraction. ICG extraction ratio was measured in five of six organ donors; it averaged 0.538 ± 0.218 (range, 0.310 to 0.909) and was not correlated with albumin or sucrose extravascular space. In cirrhotics (n = 9), ICG extraction ranged from 0.025 to 0.213 and was significantly correlated with the extravascular space accessible to albumin (Fig. 7; $r = .841$; $P < .005$), but not with that of sucrose ($r = .453$, P = NS).

DISCUSSION

Using the multiple-indicator dilution approach, we have characterized for the first time the microcirculation of normal or near-normal human livers, using isolated perfused liver preparations. The permeability of human sinusoids was found to be comparable to that of normal dog and rat livers.[5,8,16-18] The proportion of the interstitial space available varies with molecular weight of the probe, larger molecules like albumin being excluded from a substantial proportion of the space, and sucrose essentially penetrating all of the space. The labeled water penetrates the total cell space. The behavior of tracers exchanging across normal liver sinusoids differs remarkably from that seen in capillaries of the lung, heart, or brain. Capillaries in these organs are relatively impermeable to large molecules like albumin and only moderately permeable to small molecules like sucrose.[17,19,20]

In organ donors, the sinusoidal volume and the extravascular volume accessible to albumin, sucrose, and water were larger after hepatic artery than after portal vein injection. Similar observations have been reported in normal rats[13,21,22] and are best explained by an unshared arterial sinusoidal bed. When the terminal hepatic arteriolar sphincters open, arterial blood jets into the sinusoids for a certain distance before mixing with low-pressure portal blood and a segment of the sinusoids is perfused solely by arterial blood.[13,23,24] The extravascular space associated with the arterially supplied peribiliary plexus has also been shown to contribute to the excess space after hepatic artery injection.[22]

During the perfusion, the livers appeared to remain viable, as assessed by gross appearance, perfusion pressures, oxygen consumption, and clearance function, but there was evidence of ischemic injury, as shown by the release of aminotransferases in the reservoir. Cold ischemia-reperfusion injury is known to result in endothelial cell damage,[25] and this could have influenced the assessment of the liver microcirculation in our experiments. Surprisingly, cold ischemia-reperfusion injury in rats has been shown to have little or no effect on the liver microcirculation as assessed by the multiple indicator dilution technique.[26,27] In the current study, the pattern of diffusion of red blood cells, albumin, sucrose, and water in organ donors was comparable to that of normal animals, also suggesting that the micro-

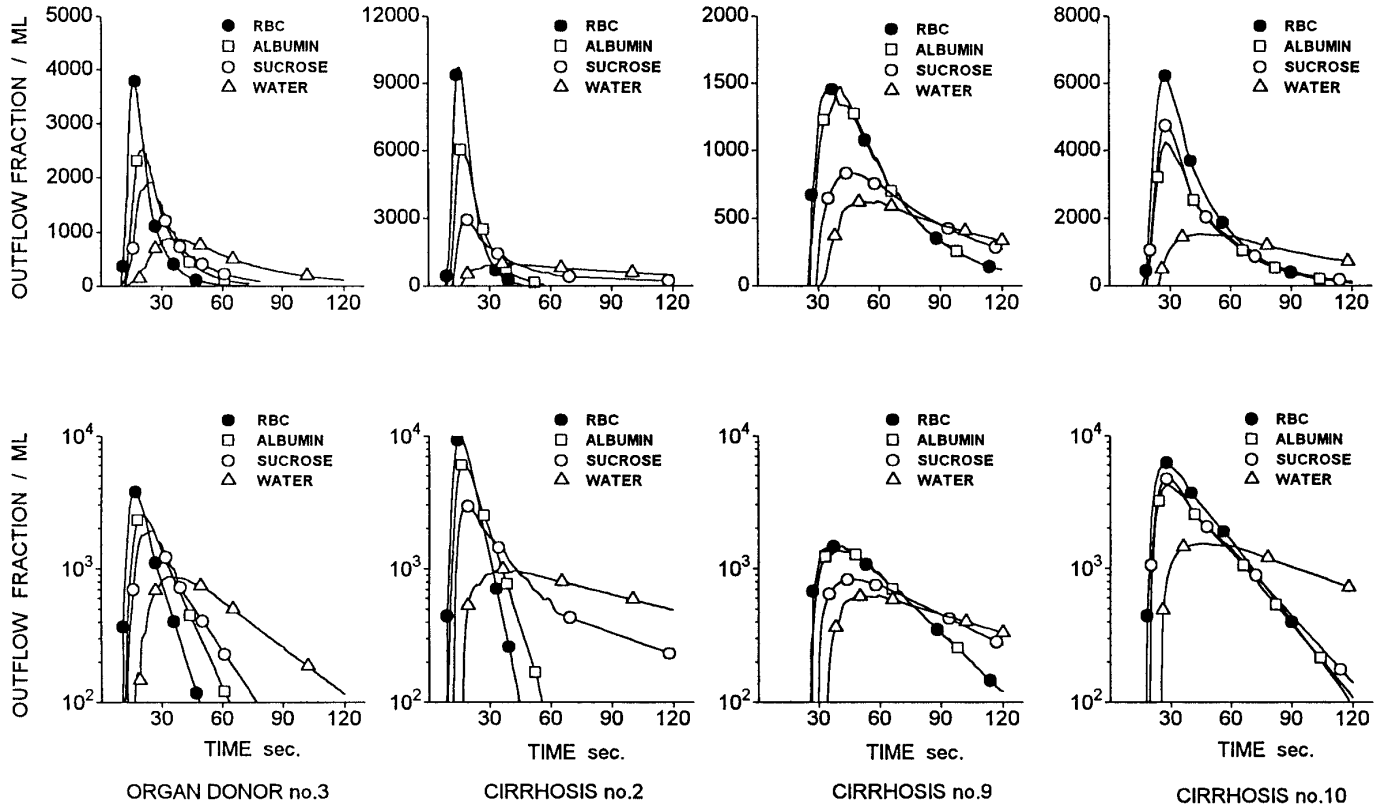

FIG. 3. Representative multiple indicator dilution curves in the outflow after portal vein injection in an organ donor and in patients with cirrhosis. In the top panel, the ordinate scale is linear; in the bottom panel, the ordinate scale is logarithmic.

circulatory abnormalities caused by cold ischemia-reperfusion were minimal.

In cirrhotic livers, studies with labeled microspheres indicated the presence of large intrahepatic shunts between the portal and hepatic veins in 8 of 10 cases, whereas there was no shunting from the hepatic artery to the hepatic veins. Shunts were absent in organ donors. The presence of shunts resulted in bimodal out-

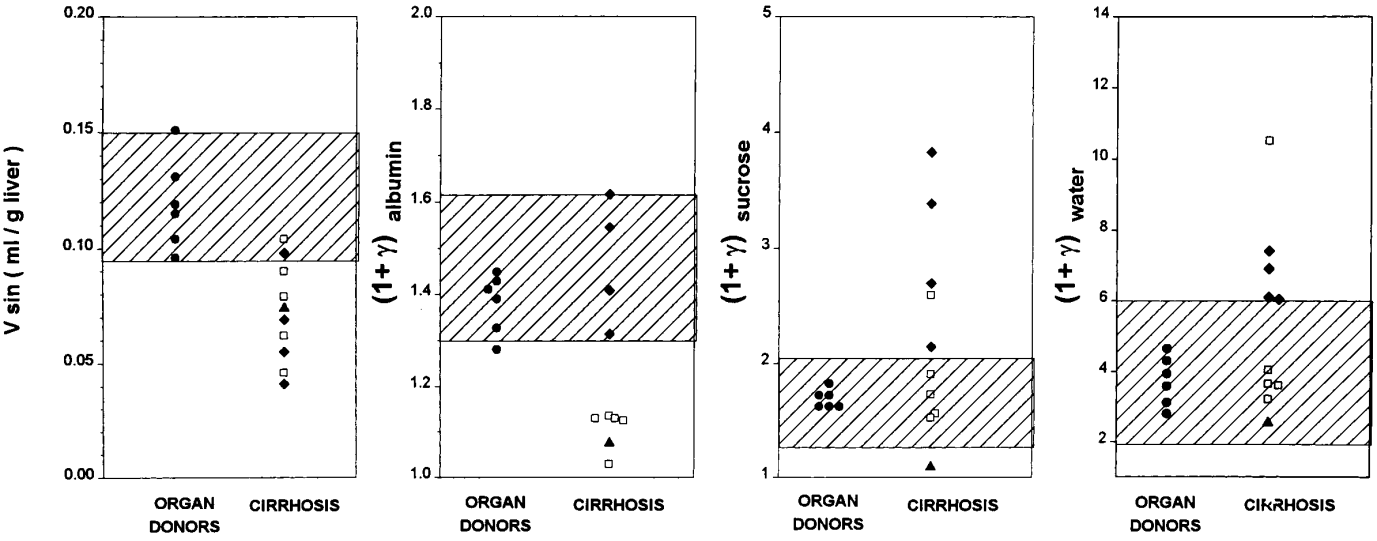

FIG. 4. Sinusoidal volume and volume accessible to albumin, sucrose, and water relative to that of red blood cells (1 + γ), after portal vein injection of tracers. The hatched area is the range of values in normal rats in our laboratory (95% confidence interval, reference 8). Cirrhosis, cases 1 to 4 ♦; cirrhosis, cases 5 to 9 □; cirrhosis, case 10 ▲.

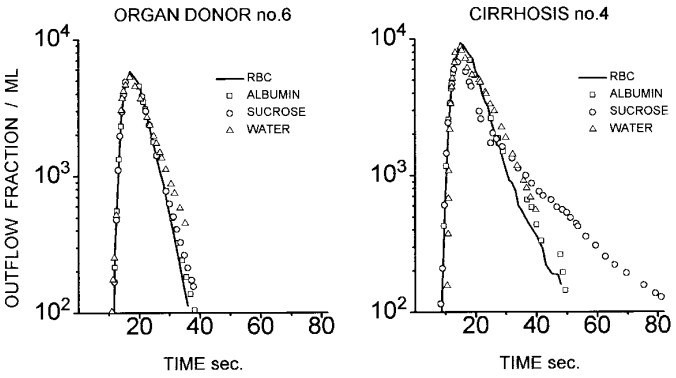

FIG. 5. Representative examples of superimposition of the transformed albumin, sucrose, and water curve on labeled red blood cells (RBC) curve in an organ donor and a patient with cirrhosis. In the cirrhotic patient, the sucrose curve could not be transformed to superimpose on the RBC curve as expected in the normal flow-limited case.

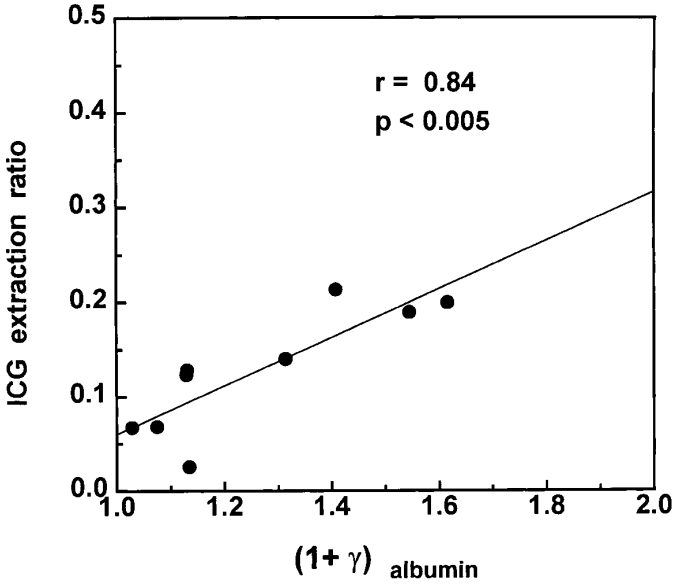

FIG. 7. Correlation between the relative volume accessible to albumin (1 + γ) and the extraction ratio of ICG in patients with cirrhosis.

flow curves for labeled red cells, albumin, sucrose, and water, with an early component related in time to the peak of microspheres, and a later component corresponding to label that has passed to a more normal part of the vascular bed. To examine the behavior of diffusible labels in the sinusoids of cirrhotic livers, the microspheres curve was therefore subtracted from each tracer curve before analysis (Fig. 2).

The sinusoidal space, expressed as milliliters per gram of liver, was decreased in cirrhotic livers. All patients had severe cirrhosis, with large amount of fibrous tissue in the liver. It is likely that the apparent decrease in sinusoidal volume is due in large part to a decrease in the hepatocyte volume fraction at the expense of connective tissue. Using the multiple-indicator dilution technique, the sinusoidal volume was also found to be decreased in rats with CCl_4-induced cirrhosis[5,8] or biliary cirrhosis,[28] but was comparable to that of controls when corrected of the decrease in hepatocyte volume fraction.[28] In human subjects, morphometric studies indicate that the sinusoidal volume relative to that of hepatocytes is comparable in normal and cirrhotic livers.[29,30]

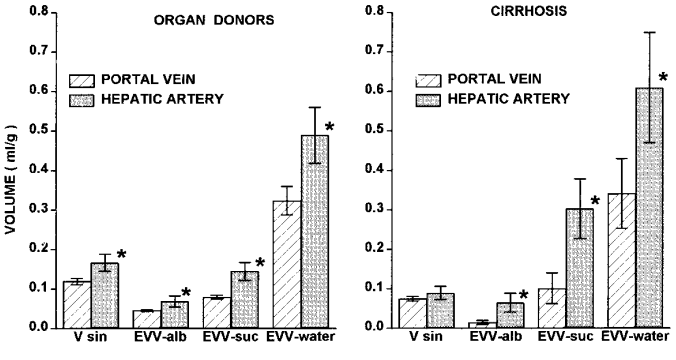

FIG. 6. Sinusoidal volume (V_{sin}) and extravascular volume (EVV) accessible to albumin, sucrose, and water after portal vein or hepatic artery injection of tracers in organ donors and patients with cirrhosis.

To avoid the difficulty in interpreting changes in extravascular volumes in the presence of fibrosis, the extravascular volumes of albumin, sucrose, and water were examined relative to that of red blood cells (1 + γ). The data suggest a pattern of evolution that is qualitatively compatible with progressive capillarization of hepatic sinusoids. In the first four cases, the diffusion of albumin in the space of Disse was normal, but the diffusion of sucrose was abnormal. Sucrose is characteristically confined to the extracellular space and, in continuous capillaries, its permeability is not large. In cases 5 to 9, the diffusion of albumin in the space of Disse was restricted, and the albumin curve tended to move toward the RBC curve. Sucrose curves exhibited a barrier-limited form, and the volume accessible to sucrose was smaller than that in the first group of patients. Finally, in case no. 10, both albumin and sucrose were confined to the vascular space. These changes are those expected when a progressive decrease in permeability occurs for substances exchanging across a microvascular bed.[18,19] Clinical data presented in Table 1 suggest that patients 5 through 10 had more severe cirrhosis than patients 1 through 4 and one can reasonably assume that capillarization increases with increasing severity of the liver disease.

The extraction ratio of ICG by the isolated perfused liver in organ donors averaged 0.538, a value comparable to or slightly lower than that reported in healthy subjects *in vivo*.[16,31,32] In cirrhotic livers, the extraction ratio of ICG was decreased, averaging 0.128 ± 0.062, and was significantly correlated with the extravascular space accessible to albumin. This correlation is similar

to that previously observed in cirrhotic patients studied *in vivo*.[9] ICG is bound to albumin,[33] and its extraction would be expected to be facilitated if the protein carrying it was able to approach the sinusoidal surface of hepatocytes. The reduced extraction of ICG in cirrhosis may thus be accounted for by capillarization of sinusoids, which impairs the access of this protein-bound dye to the liver cell surface.

In summary, using the multiple-indicator dilution approach in isolated perfused livers, we have characterized the hepatic microcirculation in normal and cirrhotic human livers. Two kinds of alterations were found in cirrhosis: intrahepatic shunts and capillarization of sinusoids with imposition of a barrier between the vascular and interstitial space. These changes restrict the access of blood solutes to the hepatocytes and contribute to liver failure irrespective of the metabolic capacity of hepatocytes.

Acknowledgment: We thank François Carrière, Lise Giroux, Jean-Luc Petit, Ginette Raymond, and Bernard Rocheleau for invaluable technical assistance, and Manon Bourcier for preparation of the manuscript.

REFERENCES

1. Wood AJJ, Villeneuve JP, Branch RA, Rogers LW, Shand DG. Intact hepatocyte theory of impaired drug metabolism in experimental cirrhosis in the rat. Gastroenterology 1979;76:1358-1362.
2. Schaffner F, Popper H. Capillarization of hepatic sinusoids. Gastroenterology 1963;44:239-242.
3. Horn T, Christoffersen P, Henriksen JH. Alcoholic liver injury: defenestration in non cirrhotic livers: a scanning electron microscopic study. HEPATOLOGY 1987;7:77-82.
4. Martinez-Hernandez A. The hepatic extracellular matrix. II. Electron immunohistochemical studies in rats with CCl_4-induced cirrhosis. Lab Invest 1985;53:166-186.
5. Varin F, Huet PM. Hepatic microcirculation in the perfused cirrhotic rat liver. J Clin Invest 1985;76:1904-1912.
6. Reichen J, Egger B, Ohara N, Zeltner B, Zysset T, Zimmermann A. Determinants of hepatic function in liver cirrhosis in the rat: multivariate analysis. J Clin Invest 1988;82:2069-2076.
7. Martinez-Hernandez A, Martinez J. The role of capillarization in hepatic failure: studies in carbon tetrachloride-induced cirrhosis. HEPATOLOGY 1991;14:864-874.
8. Gariépy L, Fenyves D, Kassissia I, Villeneuve JP. Clearance by the liver in cirrhosis II. Characterization of propranolol uptake with the multiple indicator dilution technique. HEPATOLOGY 1993;18:823-831.
9. Huet PM, Goresky CA, Villeneuve JP, Marleau D, Lough JO. Assessment of liver microcirculation in human cirrhosis. J Clin Invest 1982;70:1234-1244.
10. Goresky CA. A linear method for determining liver sinusoidal and extravascular volume. Am J Physiol 1963;204:626-640.
11. Villeneuve JP, Huet PM, Gariépy L, Fenyves D, Willems B, Côté J, Lapointe R, et al. Isolated perfused cirrhotic human liver obtained from liver transplant patients: a feasibility study. HEPATOLOGY 1990;12:257-263.
12. Kassissia I, Rose CP, Goresky CA, Schwab AJ, Bach GG, Guirguis S. Flow-limited tracer oxygen distribution in the isolated perfused rat liver: effects of temperature and hematocrit. HEPATOLOGY 1992;16:763-775.
13. Kassissia I, Brault A, Huet PM. Hepatic artery and portal vein vascularization of normal and cirrhotic rat liver. HEPATOLOGY 1994;18:1189-1197.
14. Meier P, Zierler KL. On the theory of the indicator-dilution method for measurement of blood flow and volume. J Appl Physiol 1954;6:731-744.
15. Cousineau D, Goresky CA, Rose CP, Lee S. Reflex sympathetic effects on liver vascular space and liver perfusion in dogs. Am J Physiol 1985;248:H186-192.
16. Caesar J, Shaldon S, Chiandussi L, Guevera L, Sherlock S. The use of indocyanine green in the measurement of hepatic blood flow and as a test of hepatic function. Clin Sci 1961;21:43-47.
17. Goresky CA, Rose CP. Blood-tissue exchange in livers and hearts: the influence of heterogeneity of capillary transit times. Fed Proc 1977;36:2629-2634.
18. Goresky CA, Huet PM, Marleau D, Lough JO, Villeneuve JP. Blood-tissue exchange in cirrhosis of the liver. In: Tygstrup N, Orlandi F, eds. Cirrhosis of the liver: methods and fields of research. New York: Elsevier-Science, 1987:143-164.
19. Goresky CA, Ziegler WH, Bach GG. Capillary exchange modeling: barrier-limited and flow-limited distribution. Circ Res 1970;27:739-764.
20. Ziegler WH, Goresky CA. Transcapillary exchange in the working left ventricle of the dog. Circ Res 1971;29:181-207.
21. Reichen J. Role of the hepatic artery in canalicular bile formation by the perfused rat liver. J Clin Invest 1988;81:1462-1469.
22. Pang KS, Sherman IA, Schwab AJ, Geng W, Barker F, Dlugosz JA, Cuerrier G, et al. Role of the hepatic artery in the metabolism of phenacetin and acetaminophen: an intravital microscopic and multiple-indicator dilution study in perfused rat liver. HEPATOLOGY 1994;20:672-683.
23. Rappaport AM. The microcirculatory hepatic unit. Microvasc Res 1973;6:212-228.
24. Watanabe Y, Puschel GP, Gardeman A, Jungermann K. Presinusoidal and proximal intrasinusoidal confluence of hepatic artery and portal vein in rat liver: functional evidence by orthograde and retrograde bivascular perfusion. HEPATOLOGY 1994;19:1198-1207.
25. McKeown CMB, Edwards V, Philips MJ, Harvey PRC, Petrunka CN, Strasberg SM. Sinusoidal lining cell damage: the critical injury in cold preservation of liver allografts in the rat. Transplantation 1988;46:178-191.
26. Combis JM, Semret M, Brault A, Piché D, Huet PM. The liver microcirculation during cold ischemia [Abstract]. HEPATOLOGY 1991;14:280.
27. Imamura H, Brault A, Huet PM. The hepatic microcirculation following 24 hr cold ischemia in UW solution and orthotopic liver transplantation in the rat [Abstract]. Gastroenterology 1994;106:908.
28. Ohara N, Schaffner T, Reichen J. Structure-function relationship in secondary biliary cirrhosis in the rat: stereologic and hemodynamic characterization of a model. J Hepatol 1993;17:155-162.
29. Ryoo JW, Buschmann RJ. Morphometry of liver parenchyma in needle biopsy specimens from patients with alcoholic liver disease: variables for the diagnosis and prognosis of cirrhosis. Mod Pathol 1989;172:555-559.
30. Shimizu H, Yokoyama T. Three-dimensional structural changes of hepatic sinusoids in cirrhosis providing an increase in vascular resistance of portal hypertension. Acta Pathol Jpn 1993;43:625-634.
31. Leevy CM, Mendenhall CL, Lesko W, Howard MM. Estimation of hepatic blood flow with indocyanine green. J Clin Invest 1962;41:1169-1179.
32. Skak C, Keiding S. Methodological problems in the use of indocyanine green to estimate hepatic blood flow and ICG clearance in man. Liver 1987;7:155-162.
33. Hwang SW. Plasma and hepatic binding of indocyanine green in guinea pigs of different ages. Am J Physiol 1975;228:718-724.